



## Fault Classification in Power Distribution Systems with Photovoltaic Distributed Generation Insertion

Andréia S. Santos <sup>1</sup>; Andréia B. A. Ferreira <sup>1</sup>; Paula A. Montenegro <sup>1</sup>; Lucas Teles Faria <sup>2</sup>; Carlos R. Minussi <sup>1</sup>

<sup>1</sup> Dept. of Electrical Engineering, São Paulo State University (UNESP), Ilha Solteira, São Paulo, Brazil; [andrea.faria@unesp.br](mailto:andrea.faria@unesp.br), [andrea.brasil@unesp.br](mailto:andrea.brasil@unesp.br), [paola.andrea@unesp.br](mailto:paola.andrea@unesp.br), [carlos.minussi@unesp.br](mailto:carlos.minussi@unesp.br)  
<sup>2</sup> Dept. of Energy Engineering, UNESP, Rosana, São Paulo, Brazil; [lucas.teles@unesp.br](mailto:lucas.teles@unesp.br)

### ABSTRACT

Faults detection and classification considering distributed generation insertion is a crucial procedure for power distribution systems. The significant growth of distributed generation units in the utility grid results in impacts on the conventional protection systems' operation. These impacts are mainly caused by changes in the short-circuit current's characteristics, direction, and amplitude. In this sense, this study addresses the impact of photovoltaic penetration on short-circuit fault classification process. The fault conditions are available in a modified IEEE 34-bus test system and modeled in ATPDraw. The algorithm for short-circuit fault detection and classification is developed using MATLAB programming environment. Multilayer *Perceptron* artificial neural network is used to classify short-circuits types. The accuracy rate of the fault classification algorithm reduces as long as the photovoltaic panels insertion increases, being 100% and 96.5% without photovoltaic insertion and with high photovoltaic insertion, respectively.

**Keywords:** Multilayer *Perceptron*, Power Distribution Systems, Photovoltaic panels, Short-Circuit Fault Classification.

### Introduction

Power distribution systems (PDS) are changing in recent years due to the incorporation of distributed generation (DG) resources. The arbitrary and large-scale DG penetration can impact the detecting, classifying, and locating faults processes. This impact can occur due changes in PDS topology, where its radial characteristics is losing, because there are many DG units' sources in the system. These changes challenge the effective operation of conventional protection systems [1], [2].

The massive insertion of photovoltaic (PV) DG units into PDS impacts on conventional protection systems' operation. That impact is due to its contribution to the short-circuit current. Thus, as the PV penetration in a distribution feeder increases, the fault current profiles are considerably different when compared to those ones without PV insertion. Therefore, the short-circuit currents variations can impact on protection devices' operation and coordination [3].

The PDS main purpose is supply the loads of consumer's units without interruptions. However, such systems are subject to events such as: electrical discharges, tree vegetation, system components damage, and human errors which usually cause disturbances and lead to interruptions in electricity supply [4].

In this context, short-circuit fault classification is performed in unbalanced three-phase PDS with PV panels insertion. Fault scenarios are created considering a variation in test system parameters and several levels of PV penetration. The fault classification algorithm inputs are the current signals measured at the substation output.

Several studies have been presented over the years on fault classification. In [5], the classification was performed via a Convolutional Neural Network (CNN). Three-phase currents signals were used directly as input; thus, there was not a pre-processing phase. The results achieved an average accuracy of 99.52% for all the fault cases tested.

In [6], Patcharoen and Atcharoen proposed an algorithm for classifying multiple faults considering wind power penetration. Three-phase currents signals were processed using discrete wavelet transform. They were the input set for the classifier whose precision achieved accuracy of 100% under wind power variation.



A proposal for faults detecting and classifying in a system with PV penetration was presented in [7]. The technique was based on a combination of generative adversarial networks and social spider. Sensors were implemented to measure changes in currents and voltages. The method achieved satisfactory performance with accuracy of 0.95.

## Short-Circuit Faults Classification

### A. Methodology for Short-Circuit Fault Classification

Fault classification is performed by analyzing the changes in the current signals amplitude after its occurrence in the electrical system. The disturbed phases have magnitude of currents higher than those ones operating under normal conditions. As a result, the average of faulted phases currents will be higher than those ones operating under normal conditions. In this way, the distinct characteristics of fault types can be extracted by average of current signals. Once a fault is detected in PDS, the classification step is activated. According to [8], there is a data window consisting of two samples cycles of post-fault current signals measured at substation output. Thus, one can obtain the average current of each phase using (1)-(2).

$$M_i = \frac{\sum x_i}{N}, \text{ with } i \in abc \text{ phases} \quad (1)$$

$$\mathbf{M} = [M_a \quad M_b \quad M_c] \quad (2)$$

Where  $M_i$  is the average of current signals for each phase  $i$  and  $x_i$  represents the  $n$ th sample of current signals for the phase  $i$  and  $N$  is the number of signals.

The normalized averages  $\bar{M}_i$  obtained via (3) are applied as classifier's input.

$$\bar{M}_i = \frac{M_i}{\sum \mathbf{M}}, \text{ with } i \in abc \text{ phases} \quad (3)$$

Where  $\sum \mathbf{M}$  is the sum of the  $\mathbf{M}$  vector's elements in (2). The phases with anomalies have higher normalized averages than those ones operating under nominal conditions; therefore, it possible to determine the operating status of each phase.

### B. Short-Circuit Classification

The short-circuit classification is performed by multilayer *perceptron* (MLP) artificial neural networks with backpropagation supervised training algorithm, as presented in [9].

The classification process is divided into two stages. In the former, defective phases are identified using the outputs provided by MLP. Binary values are assigned to phases that are not within a pre-established threshold  $\mathcal{L}_i$ , according to (4). The absence of an anomaly is represented by bit 0, while short-circuited phase is represented by bit 1.

$$S_i = \begin{cases} 0, & \text{Phase}_i \text{ State} \leq \mathcal{L}_i \text{ where } i \in \{a, b, c\} \\ 1, & \text{otherwise} \end{cases} \quad (4)$$

The latter step consists of counting faulty phases using (5). The short-circuit type is determined via number of short-circuit phases.

$$\text{Short - Circuit Type} = \begin{cases} \text{single - phase,} & \text{if } \sum_{i=1}^3 S_i = 1 \\ \text{two - phase,} & \text{if } \sum_{i=1}^3 S_i = 2 \\ \text{three - phase,} & \text{if } \sum_{i=1}^3 S_i = 3 \end{cases} \quad (5)$$



## Results

### A. Test System Modelling IEEE-34 Bus

The fault conditions are simulated on modified IEEE-34 bus test system and modeled using the ATP and its ATPDraw graphic interface [10]. The system consists of single-phase and three-phase branches, and it has a nominal voltage of 24.9 kV. The loads are modeled as a constant impedance model and the voltage regulators are removed. Four scenarios with different levels of PV penetration are created according [10]. In the first scenario, the classification of fault types is performed without PV panels; in the others three scenarios, PV panels are introduced with installed power of 1 MW (one PV panel), 2 MW (two PV panels), and 3 MW (three PV panels), respectively.

The MLP algorithm is implemented in MATLAB<sup>®</sup> programming environment. All simulations are performed on a computer with an Intel Core i7 processor; 1.8–1.99 GHz and 8 GB of RAM.

### B. Short-Circuit Fault Classification

MLP topology applied in this study has three neural layers. The input layer contains three neurons, and it receives the normalized averages as input vector. The MLP structure has a single hidden layer with ten neurons. Finally, the output layer contains three neurons. The classification process aims to identify the faulty phases. Operating status of each phase is provided by MLP outputs. Several fault conditions performed considering variations in the system parameters, as shown in Table 1.

In each scenario, there are 2244 simulations, amounting 8976 simulations in total. Training phases apply 70% of data, equivalent to 6284 simulations, while the remaining 30%, equivalent to 2692 simulations is allocated for MLP testing and validation. Three MLP are introduced, one for each short-circuit type to maximize the accuracy rate.

Short-circuit classifications for the four scenarios are shown in Fig. 1. In Fig. 1 (a), first scenario shows accuracy of 100% for all short-circuits. However, Fig. 1 (b), second scenario, the single-phase short-circuit shows an error of 1.5%, while the single-phase and two-phase shorts-circuits maintained the same accuracy at first scenario. In third scenario Fig. 1. (c), there is a reduction of accuracy rate for two-phase short-circuits of 0.5, while single-phase and three-phase short-circuits reach accuracy rate equal to 100%. In the last scenario Fig. 1 (d), single-phase and two-phase short-circuits show errors of 3.5% and 2.5%, respectively. Three-phase shorts-circuit; on the other hand, maintain an accuracy of 100%.

Thus, there are changes in current levels after PV panels insertion especially in the buses furthest from the substation, such as bus 860. Be a single-phase short-circuit in phase  $B_g$ , which occur at bus 860. The normalized average obtained without PV penetration is equal to  $\bar{M} = \{0.16, 0.73, 0.11\}$ . After three PV panels insertion, these values change significantly. The shorted-circuit phase currents become very close than those ones in the  $A$  and  $B$  with normal phases. As a result, three phase averages become very close to  $\bar{M} = \{0.30, 0.38, 0.32\}$ . In some cases, in scenario 3, the average of shorted-circuit phase becomes very close or lower than, those ones in phases without anomalies. Therefore, the PV panels insertion on PDS can leading to an incorrect classification of short-circuit phases.

Table 1. System parameters.

Parameters	Configurations
Fault types	$A_g, B_g, C_g, AB, AC, BC, AB_g, AC_g, BC_g, ABC, ABC_g$
Fault Location (buses)	802, 806, 814, 828, 830, 850, 854, 860
DG Units	1 PV panel (at buses 822, 840, and 848)
Fault resistance	1Ω to 40Ω
Fault inception	0°, 45°, 90°, and 120°

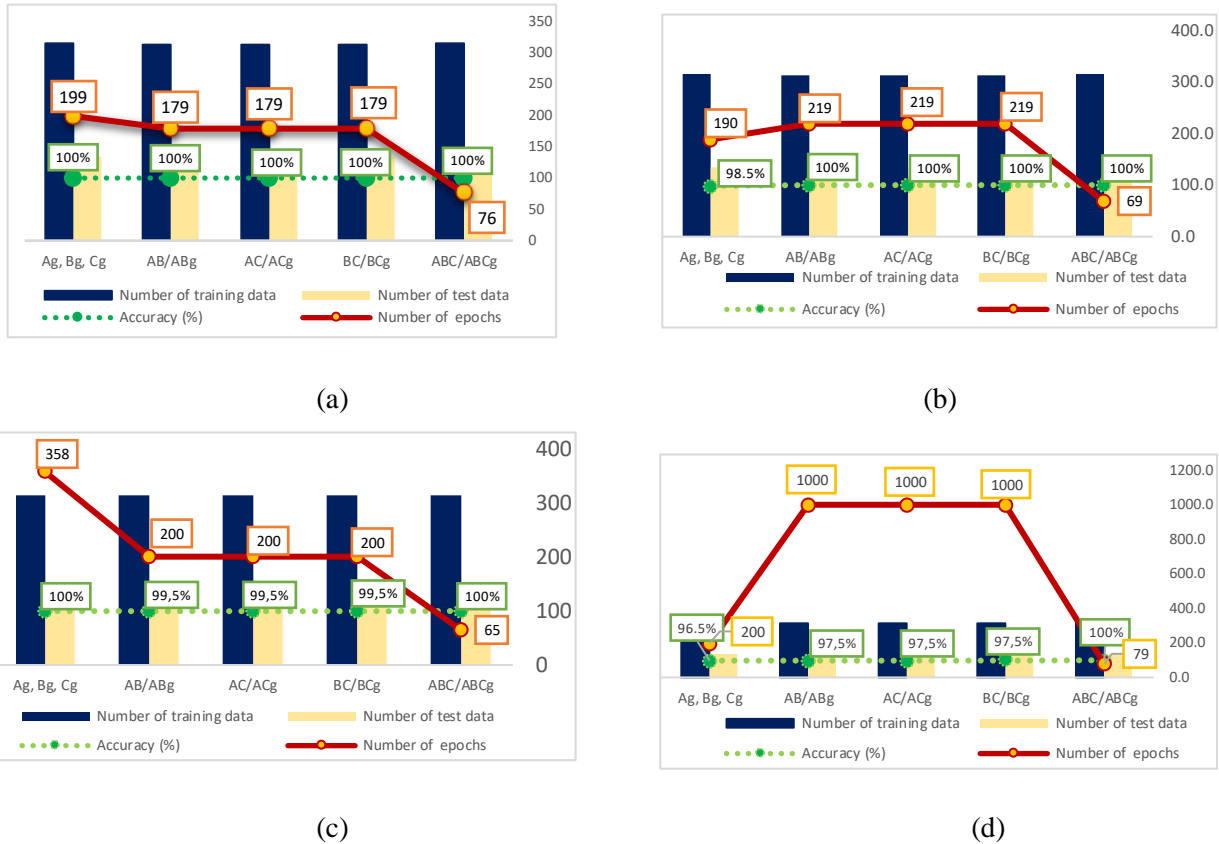


Figure 1 – Classification and accuracy for four scenarios: (a) without PV panels (scenario 1); (b) one PV panel (scenario 2); (c) two PV panels (scenario 3); and (d) three PV panels (scenario 4).

### C. Validation

Classifier validation is performed for short-circuits with accuracy less to 100%. An MLP neural network is introduced for each fault type. In Table 2, the confusion matrices corresponding to scenarios 2, 3 and 4 are presented.

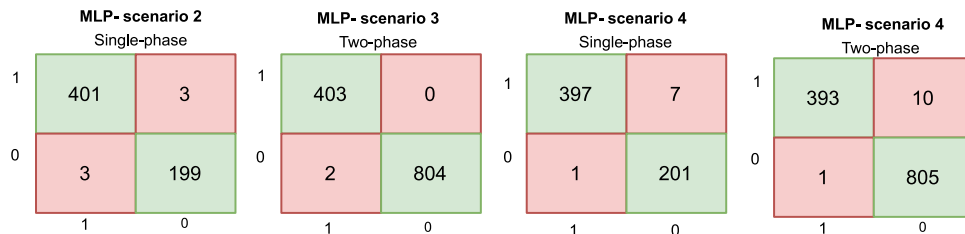


Figure 2 – Confusion matrix for scenarios 2, 3 and 4.

Statistical metrics such as precision, recall and F1-score calculated via (6), (7) and (8) are incorporated to evaluate the classifier system. These metrics are obtained from the confusion matrix that includes two classes: short-circuit and normal. Table 2 shows the classification performance for scenarios 2, 3 and 4.

$$Precision = \frac{Q_{NN}}{Q_{NN} + Q_{FN}} \quad (6)$$

$$Recall = \frac{Q_{NN}}{Q_{NN} + Q_{NF}} \quad (7)$$

$$F1 - Score = \frac{2(Precision \times Recall)}{(Precision + Recall)} \quad (8)$$



Table 2 – Classifier performance for scenarios 2 ,3. and 4.

Classifier	Scenario	Recall	Precision	F1-Score
Single-Phase	2	0.9926	0.9926	0.9926
Two-Phase	3	1.0000	0.9951	0.9975
Single-Phase	4	0.9827	0.9975	0.9900
Two-Phase	4	0.9777	0.9975	0.9875

## Conclusion

This study addressed the impact of photovoltaic (PV) panels insertion on short-circuit fault classification process in unbalanced power distribution system (PDS). Three-phase currents measured at the substation output were analyzed. Short-circuit classification was performed via three multilayer *perceptron* (MLP) artificial neural network. The fault classification accuracy for different scenarios were satisfactory. The assertiveness rate for the scenarios 1, 2, 3, and 4 were equal to 100%, 98.5%, 99.5%, and 96.5%, respectively. These results showed the impact of PV panels insertion in PDS, where they contribute to changes in short-circuit currents levels.

## Acknowledgment

This research was funded by Coordination for the Improvement of Higher Education Personnel (CAPES), Financing Code 001, and National Council for Scientific and Technological Development (CNPq).

## References

- [1] A. M. El-Zonkoly, "Fault diagnosis in distribution networks with distributed generation," *Electric Power Systems Research*, vol. 81, no. 7, pp. 1482–1490, Jul. 2011, doi: 10.1016/j.epsr.2011.02.013.
- [2] S. F. Alwash, V. K. Ramachandaramurthy, and N. Mithulananthan, "Fault-location scheme for power distribution system with distributed generation," *IEEE Transactions on Power Delivery*, vol. 30, no. 3, pp. 1187–1195, Jun. 2015, doi: 10.1109/TPWRD.2014.2372045.
- [3] H. Hooshyar and M. E. Baran, "Fault analysis on distribution feeders with high penetration of PV systems," *IEEE Transactions on Power Systems*, vol. 28, no. 3, pp. 2890–2896, 2013, doi: 10.1109/TPWRS.2012.2227842.
- [4] S. S. Gururajapathy, H. Mokhlis, and H. A. Illias, "Fault location and detection techniques in power distribution systems with distributed generation: A review," *Renewable and Sustainable Energy Reviews*, vol. 74. Elsevier Ltd, pp. 949–958, 2017. doi: 10.1016/j.rser.2017.03.021.
- [5] P. Rai, N. D. Londhe, and R. Raj, "Fault classification in power system distribution network integrated with distributed generators using CNN," *Electric Power Systems Research*, vol. 192, Mar. 2021, doi: 10.1016/j.epsr.2020.106914.
- [6] T. Patcharoen and A. Ngaopitakkul, "Fault classifications in distribution systems consisting of wind power as distributed generation using discrete wavelet transforms," *Sustainability (Switzerland)*, vol. 11, no. 24, Dec. 2019, doi: 10.3390/su11247209.
- [7] H. Cao, H. Zhang, C. Gu, Y. Zhou, and X. He, "Fault detection and classification in solar based distribution systems in the presence of deep learning and social spider method," *Solar Energy*, vol. 262, Sep. 2023, doi: 10.1016/j.solener.2023.111868.
- [8] A. da S. Santos, L. T. Faria, M. L. M. Lopes, A. D. P. Lotufo, and C. R. Minussi, "Efficient Methodology for Detection and Classification of Short-Circuit Faults in Distribution Systems with Distributed Generation," *Sensors*, vol. 22, no. 23, Dec. 2022, doi: 10.3390/s22239418.
- [9] D. E. Rumelhart, G. E. Hinton, and Williams Ronald J, "Learning representations by back-propagating errors," *Nature*, vol. 323, no. 6088, pp. 533–536, 1986.
- [10] H. K. Høidalen, L. Prikler, and F. Peñaloza, "ATPDRAW version 7.3." pp. 1–362, May 2021.